Feature Detection Based Spectrum Sensing in NOMA System

Jingyi Wu[1], Tianheng Xu[1,2], Ting Zhou[1(✉)], and Kaijie Wang[1]

[1] Shanghai Advanced Research Institute, Chinese Academy of Sciences, Shanghai 201210, China
{wujy,xuth,zhouting,wangkaijie2019}@sari.ac.cn
[2] Shanghai Frontier Innovation Research Institute, Shanghai, China

Abstract. Non-orthogonal multiple access (NOMA) technology allows multiple users to share the same spectrum resource. Meanwhile, the technology of spectrum sensing enables us to find the free time of the spectrum. Both two technologies can significantly improve spectrum efficiency. In this paper, we attempt to combine the two techniques, for meeting the higher demand of spectrum resources requirements in future communication. We propose a transceiver architecture by the combination of two techniques. And we verify the feasibility of this scheme. The experiments and obtained data reveal that the proposed method is feasible. And it manifests to have a good detection performance.

Keywords: NOMA · Spectrum sensing · Feature detection · Cyclic delay diversity

1 Introduction

In the past ten years, wireless communication technology has developed rapidly, and the fifth-generation (5G) wireless communication network is currently in use [1–3]. It is supposed to have higher transmission speeds and can handle more complex scenarios [4,5]. However, for the significant growth of spectrum demands, available spectrum resources are still insufficient [6–8]. Hence, the problem of how to improve the utilization of the spectrum is a long-term challenge.

Spectrum sensing is one of the promising schemes to improve spectrum utilization [9–11]. It aims to find the spectral idle time of the primary user (PU), and allow the secondary user (SU) to share the spectrum hole dynamically [12]. The main methods of spectrum sensing include feature detection [13], energy detection [14,15] and matched filtering detection [16]. Among them, feature detection is a method that can detect the state of multiple users [17], which is used in this paper.

Meanwhile, until 5G, orthogonal multiple access (OMA) technology is the main method of information transmission. But the next generation communication technology needs to consider a more complex transmission environment

C. T. Calafate et al. (Eds.): MONAMI 2021, LNICST 418, pp. 201–217, 2022.
https://doi.org/10.1007/978-3-030-94763-7_16

and better transmission performance [18,19]. Many studies have shown that non-orthogonal multiple access (NOMA) is a very promising technology [20–22]. NOMA utilizes superposition coding at the transmitters and successive interference cancellation at the receivers to enables multiple users to multiplex on the same subchannel [23–25].

Hence, both spectrum sensing and NOMA can increase resource utilization. However, by the definition of NOMA, combining spectrum sensing with it differs much from combining with OMA. How to combine NOMA with spectrum sensing, are the problems that we pay attention to. Meanwhile, most of the existing relevant studies regard edge users as PU, center users as SU, and SU plays the role of relay for PU transmission [26–28]. For instance, Jia et al. [29] let SU play the role of the user relay, and the SU adopts the energy detection technique of spectrum sensing to identify the spectrum holes. Through theoretical derivation and simulation, they prove that their scheme has higher throughput. In the work of Wang et al. [30], SUs harvest wireless energy and sense the spectrum state simultaneously, in order to maximize the energy efficiency of the network. These studies above have done meaningful work on the combination of NOMA and spectrum sensing. However, there is still lacking research that examines the transmission status of both two NOMA users by feature detection. Hence, to answer the questions above, we attempt to explore how to set the sensing threshold under the condition of NOMA. To solve these problems, we have the following contributions in this paper:

- Firstly, we propose a feature detection based spectrum sensing technology in NOMA system, and design the system framework.
- Secondly, we verify the feasibility of this scheme. We design two patterns for detection under NOMA, and deduce the relationship between false-alarm probability (P_f) and threshold. Then we analyze the performance and compare it with that of OMA.
- Finally, We have sufficient simulations and then analyze the results. We conclude that the proposed scheme is better than OMA under the same conditions.

The remainder of this paper can be organized as follows. In Sect. 2, the system model of the spectrum sensing in NOMA is set up. Section 3 presents how the receiver gets the feature of the signal and the derivation of false alarm probability. In Sect. 4, a scheme of two users with the same working state is simulated. Section 5 discusses the situation when one user keeps on transmitting. Finally, conclusions are given in Sect. 6.

2 System Model

In this paper, we consider the model of downlink NOMA with a base station (BS) and two users, as shown in Fig. 1.

We apply cyclic delay diversity (CDD) to generating the feature of the signal. CDD uses multiple antennas to obtain signal feature [31,32]. The main transmission structure is shown in Fig. 2. In our paper, a model with two transmitting antennas and a single receiving antenna is utilized.

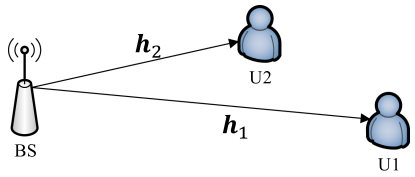

Fig. 1. The downlink system

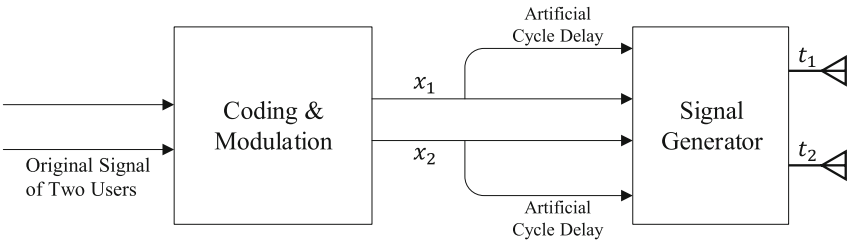

Fig. 2. Transmitter architecture for two users

We assume that x_1 and x_2 are the transmitted signals of two users respectively. The power allocation for users is α_1 and α_2, where $\alpha_1, \alpha_2 > 0$ and $\alpha_1 + \alpha_2 = 1$. The first antenna outputs two modulated signals x_1 and x_2, and the second antenna outputs x_1 and x_2 with different delays. The signals sent by two antennas are both in NOMA mode, then they pass through Rayleigh channels $\mathbf{h}$ and the signals are obtained by the receiver. The received signal by User 1 can be written as

$$r_1(n) = \mathbf{h}_1 \mathbf{t}(n) + w(n), \tag{1}$$

where $\mathbf{h}_1 = [h_{11}, h_{12}]$, $\mathbf{t}(n) = [t_1(n), t_2(n)]^T$, and $w(n)$ is the additive white Gaussian noise (AWGN) with specific power. h_{11} and h_{12} are the channel coefficients between two antennas and the receiver U1, and the difference between them is fixed. t_1 and t_2 are the signals transmitted by two antennas respectively, which can be computed by the following formulas

$$t_1(n) = \alpha_1 x_1(n) + \alpha_2 x_2(n) \tag{2}$$

and

$$t_2(n) = \alpha_1 x_1(n + d_1) + \alpha_2 x_2(n + d_2), \tag{3}$$

where d_1 and d_2 is the cyclic delay of two users respectively, which are chosen differently.

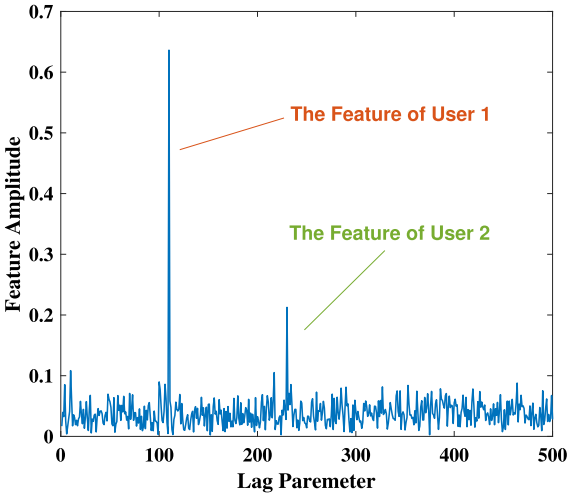

Fig. 3. The feature amplitude of NOMA signal after passing Rayleigh channel. System conditions: $SNR_1 = 0\,\text{dB}$, $SNR_2 = 5\,\text{dB}$, $\alpha_1 = 0.8$, $d_1 = 110$ and $d_2 = 230$.

3 The Proposed Method of Feature Detection in NOMA

3.1 Framework of the Receiver

We take the correlation between the received signal and the signal after its cyclic delay as the detection target, which is

$$R(\delta) = \frac{1}{S}\sum_{n=0}^{S-1} r(n)r^*(n+\delta), \tag{4}$$

where S is the length of the received signal, the symbol $(\cdot)^*$ means the conjugate operation. The correlation value reaches a maximum when δ equals the delay of the users. We call this peak the amplitude of the feature.

Take a NOMA downlink model with spectrum sensing as an example. The system satisfies: $SNR_2 - SNR_1 = 5$ dB, $SNR_1 = 0$ dB and $\alpha_1 = 0.8$. And we set the delays as $d_1 = 110, d_2 = 230$. We call User 1 the strong user. Figure 3 shows the feature amplitude of this situation.

It can be seen that there are obvious peaks at the delays of the signals, meanwhile, at other δ, the amplitude fluctuates within a small range.

3.2 Principle of Feature Detection

In spectrum sensing, the sensing process needs to determine whether the correlation at the delay (d_1, d_2) is greater than the given threshold, which is a binary decision problem. If the correlation is greater than the threshold, then we can conclude that the user is at the state of transmitting signals (denoted as H_1),

otherwise, the user is supposed not to be transmitting signals (denoted as H_0). The received signal can be written as

$$r(n) = \begin{cases} w(n), & H_0, \\ \mathbf{ht}(n) + w(n), & H_1. \end{cases} \tag{5}$$

The decision can be expressed as:

$$\begin{cases} \hat{H_0} : |R| < \lambda, \\ \hat{H_1} : |R| \geq \lambda, \end{cases} \tag{6}$$

where λ is the threshold we choose, and $\hat{H_1}$, $\hat{H_0}$ are the two possible detection results of the transmitting state. The detection probability (P_d) is the probability of correctly find the existence of the transmitter. And the false-alarm probability (P_f) is the probability of deciding the state of the transmitter to be working when it is not. Thus we have

$$\begin{aligned} P_d &= Pr(\hat{H_1}|H_1) \\ &= Pr(|R| \geq \lambda) \\ &= Pr(|\tfrac{1}{S}\textstyle\sum_{n=0}^{S-1} r(n)r^*(n+\delta)| \geq \lambda) \end{aligned} \tag{7}$$

and

$$\begin{aligned} P_f &= Pr(\hat{H_1}|H_0) \\ &= Pr(|\tfrac{1}{S}\textstyle\sum_{n=0}^{S-1} w(n)w^*(n+\delta)| \geq \lambda). \end{aligned} \tag{8}$$

3.3 False Alarm Probability Derivation

The noise is subject to Rayleigh distribution and without loss of generality, can be expressed as

$$\begin{cases} w(n) = \frac{N_0}{\sqrt{2}} w_1, \\ w(n+\delta) = \frac{N_0}{\sqrt{2}} w_2, \end{cases} \tag{9}$$

where w_1, w_2 are independent identically distributed variables subject to the standard normal distribution. To be specific,

$$\begin{cases} w_1 = x_1 + iy_1, \\ w_2 = x_2 + iy_2, \end{cases} \tag{10}$$

where x_1, x_2, y_1, y_2 satisfy

$$\begin{cases} x_1, x_2 \sim N(0,1), \\ y_1, y_2 \sim N(0,1). \end{cases} \tag{11}$$

Multiply w_1 and the conjugate of w_2, we get

$$F = w_1 w_2^* = (x_1 x_2 + y_1 y_2) + i(x_2 y_1 - x_1 y_2). \tag{12}$$

Let I and Q represent real and imaginary parts of F. Hence

$$\begin{cases} \mu_I = \mu_Q = 0, \\ \sigma_I^2 = \sigma_Q^2 = 2. \end{cases} \tag{13}$$

Suppose the length of the signal is S, accumulate all of the $w_1 w_2^*$. Then we have $\dot{F}$ as the function of the signal correlation

$$\dot{F} = \sum_{j=0}^{S-1} (I_j + iQ_j) = \dot{I} + i\dot{Q}, \tag{14}$$

where $\dot{I}, \dot{Q}$ are the real and imaginary part of $\dot{F}$, respectively. By Law of Large Numbers,

$$\begin{array}{l} \lim\limits_{S\to\infty} \frac{I - S\mu_I}{\sqrt{S}\sigma_I} \sim N(0,1), \\ \lim\limits_{S\to\infty} \frac{Q - S\mu_Q}{\sqrt{S}\sigma_Q} \sim N(0,1). \end{array} \tag{15}$$

If the length of the received signal S is large enough, we can get

$$\dot{I}, \dot{Q} \sim N(0, 2S). \tag{16}$$

$\dot{F}$ also follows the Rayleigh distribution, let $t = |\dot{F}|$, and the probability distribution can be expressed as

$$f(t) = \frac{t}{2S} e^{\frac{-t^2}{4S}} (t \geq 0). \tag{17}$$

Hence, the sum of the correlations for the noise is

$$\left| \frac{1}{S} \sum_{n=0}^{S-1} w(n) w^*(n+\delta) \right| = \frac{N_0^2}{2S} \left| \dot{F} \right|. \tag{18}$$

Then the P_f can be evaluated by

$$\begin{aligned} P_f &= Pr(|\tfrac{1}{S} \textstyle\sum_{n=0}^{S-1} w(n) w^*(n+\delta)| \geq \lambda) \\ &= Pr(\tfrac{N_0^2}{2S} |\dot{F}| \geq \lambda) \\ &= Pr(|\dot{F}| \geq \tfrac{2S\lambda}{N_0^2}) \\ &= \textstyle\int_{\frac{2S\lambda}{N_0^2}}^{+\infty} e^{\frac{-t^2}{4S}} dt \\ &= e^{-\frac{S\lambda^2}{N_0^4}}. \end{aligned} \tag{19}$$

Therefore, we get the relationship between P_f and λ it as

$$\lambda = \sqrt{-\frac{lnP_f}{S}} N_0^2. \tag{20}$$

Use the formula to determine the threshold of spectrum sensing in OMA scene, and can obtain the correctness of it. We compare this result of OMA with that of our proposed method in NOMA.

Table 1. Simulation parameters.

Parameters	Values
Original signal size	4096
Channel coding	LDPC
Coding rate	449/1024
Antenna configuration	2×1
Channel model	Rayleigh fading
Modulation	QPSK
Number of multiplexed NOMA users	2
NOMA mode	Downlink
Proportion of power distribution	$\alpha_1 : \alpha_2 = 2:1, 4:1, 10:1$
SNR difference	$SNR_2 - SNR_1 = 5$ dB

4 Simulation Results and Performance Analysis

We considered two modes of spectrum sensing in NOMA, one of which is two users share the same transmission state, the other is keep U2 transmitting.

4.1 Mode 1: Same Transfer State

Suppose strong and weak users share the same transmission state in the NOMA-spectrum sensing system. In other words, both users are transmitting signals or neither of them. Because of this limitation, this mode is more suitable for some downlink NOMA scenarios and applications. The feature amplitude of the received signal is calculated and compared with the threshold. Then we use the Monte-Carlo simulation to calculate the probability. The basic simulation parameters are listed in Table 1.

In this paper, we use two kinds of methods to calculate SNR. The first one adds the power of the two users as the power of the signal. The other one utilizes the power of a single user for its own SNR, who called "with SNR compensation". In order to give consideration to the actual conditions and fairness of the results, and to give a more complete show of the performance of the system, both methods will be used in the simulation.

We choose three power allocation rates that are widely adopted in the NOMA system [24]. They are $\alpha_1 : \alpha_2 = 2:1$, $4:1$ and $10:1$.

Figure 4 shows the detection probability P_d and false-alarm probability P_f of the two users with power allocation $\alpha_1 : \alpha_2 = 2:1$. The U1 in figs means the strong user, and the U2 means the weak user. We can see that the P_f of two users are both stay around 0.1. Figure 4(a) describes that at system SNR, the P_d curve of U2 is clearly below that of U1. At about –5 dB, the P_d of U1 reaches 0.9, meanwhile the P_d of U2 is round 0.72. This result reveals that, when the two users are at the same environment of SNR, the detection performance of weak users

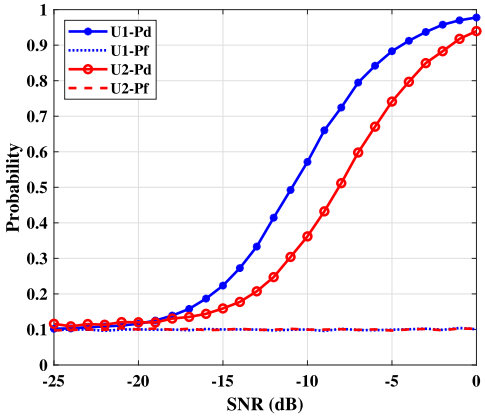

(a) The P_d and P_f of two users without SNR compensation.

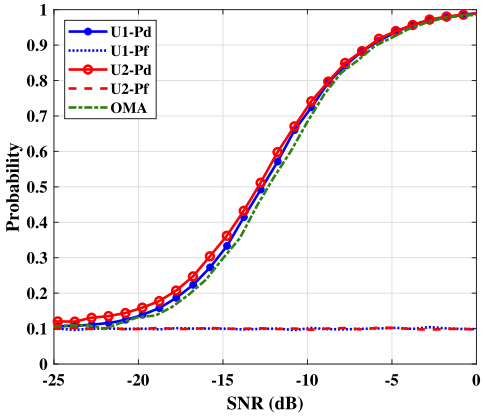

(b) The P_d and P_f of two users with SNR compensation.

Fig. 4. Downlink NOMA system with power allocation $\alpha_1 : \alpha_2 = 2 : 1$.

will be relatively weak. As we can observe from Fig. 4(b), after compensating SNR to their own SNR, both P_d of two users are almost superposed with the OMA result. It shows their P_d reach 0.9 at around –6 dB, and at 0 dB P_d nearly achieve to 1.

Then we try to simulate systems with different power allocations.

Figure 5 and Fig. 6 show the detection performance with $\alpha_1 : \alpha_2 = 4 : 1$ and $\alpha_1 : \alpha_2 = 10 : 1$, respectively. It is observed from Fig. 5(a) and Fig. 6(a) that the less power of U2 is allocated, the greater the difference between its P_d and that of the U1. When $\alpha_1 : \alpha_2 = 2 : 1$, the difference of P_d between two users is about 0.2 at most. At the same time, when $\alpha_1 : \alpha_2 = 10 : 1$, the gap can even achieve more than 0.5. It can be perceived that from either Fig. 5(b) and Fig. 6(b), after

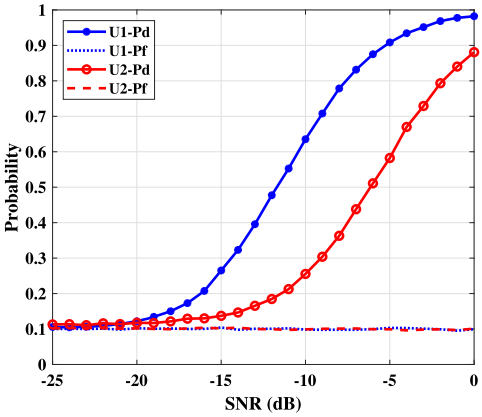

(a) The P_d and P_f of two users without SNR compensation.

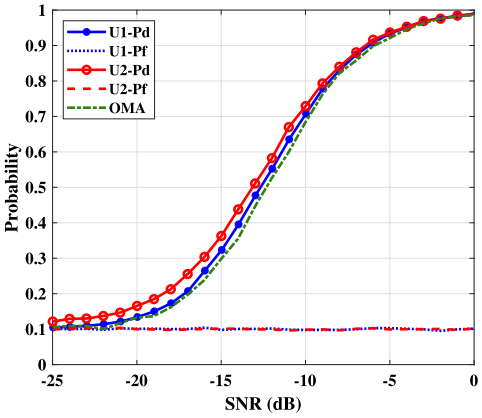

(b) The P_d and P_f of two users with SNR compensation.

Fig. 5. Downlink NOMA system with power allocation $\alpha_1 : \alpha_2 = 4 : 1$.

compensating SNR to their own SNR, in the range of approximately –8 dB to 0 dB, the detection performance of the two users remained consistent with OMA. However, when U2 is distributed less power, at low SNR, P_d of U2 will be larger than that of U1.

Combined with three groups of pictures, it can be analyzed that, transmitting with another NOMA user, the performance of U1 will not be significantly inferior to the OMA scheme. Meanwhile, the performance of U2 largely depends on the power allocation. At the same SNR, U2 is inferior to U1 as to the P_d. However, at their own SNR, the detection performance of two users is similar to that of OMA. Therefore, it is better to make the difference between α_1 and α_2 as small as possible, due to the inferiority of U2 at the same SNR.

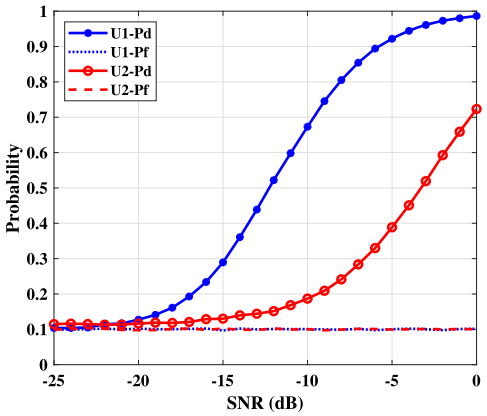

(a) The P_d and P_f of two users without SNR compensation.

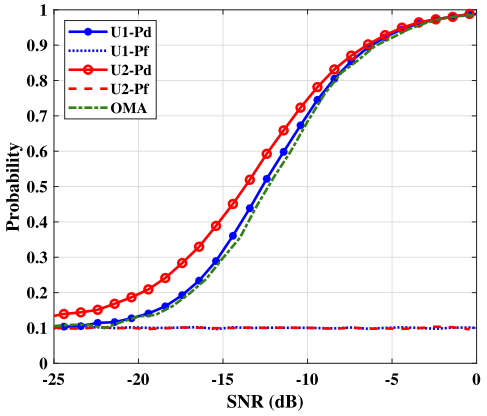

(b) The P_d and P_f of two users with SNR compensation.

Fig. 6. Downlink NOMA system with power allocation $\alpha_1 : \alpha_2 = 10 : 1$.

4.2 Mode 2: Weak User Keep Transmitting

To make the scenario more general, now keep the U2's signal always transmitting. This mode is recommended to apply to the uplink system, and we consider detecting the state of U1.

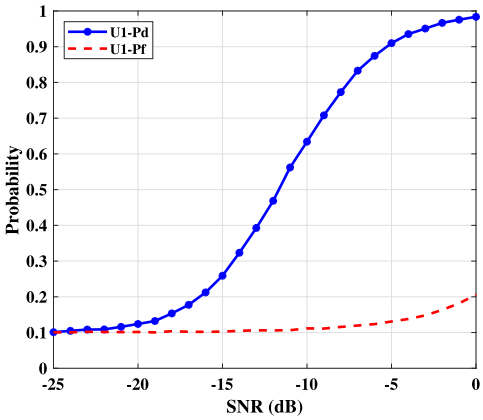

(a) The P_d and P_f of two users without SNR compensation.

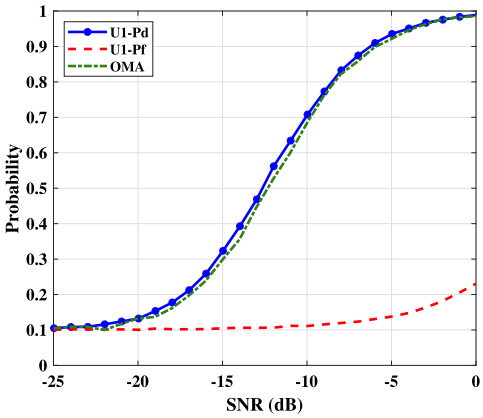

(b) The P_d and P_f of U1 with SNR compensation.

Fig. 7. Downlink NOMA system with power allocation $\alpha_1 : \alpha_2 = 4 : 1$, when U2 is keep on transmitting.

As Fig. 7 indicates, P_f starts to increase when SNR is –10 dB. And at 0 dB, P_f reaches to more than 0.2. Meanwhile, the curve of P_d is a little superior to that of OMA at some SNR.

While running the Monte-Carlo simulation, we save the mean value of the signal feature amplitude when U1 is not transmitting. Finally, output the trend of the ratio of it to the threshold when SNR changes, as is shown in Fig. 8. The straight line in the figure is the reference value of the ratio when P_f is maintained at 0.1.

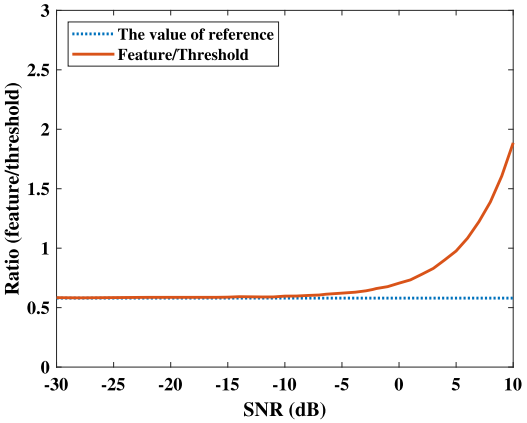

Fig. 8. The rate of the feature amplitude when U1 in H_0 condition to the threshold, with $\alpha_1 : \alpha_2 = 4 : 1$.

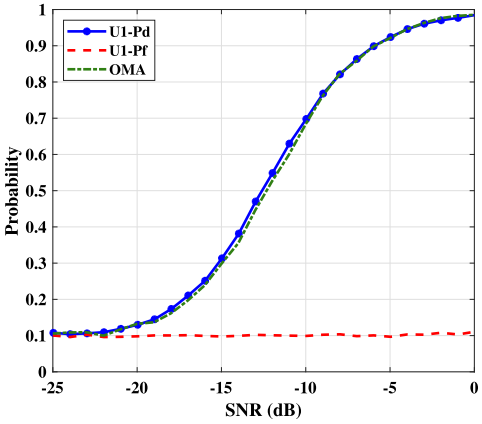

Fig. 9. Downlink NOMA system with power allocation $\alpha_1 : \alpha_2 = 4 : 1$ after threshold adjustment, when U2 is keep on transmitting.

When the power of the noise is reduced, the power of U2 is relatively increased. Therefore, Fig. 8 describes that when SNR increases, the correlation of U2 signals has a greater impact on the detection results.

We suspect that the existence of the U2 signal prevents P_f from being maintained at 0.1. In this case, not only noise but also U2 signal correlation should be considered in the P_f calculation. Hence, we need to adjust the threshold and restore P_f to 0.1.

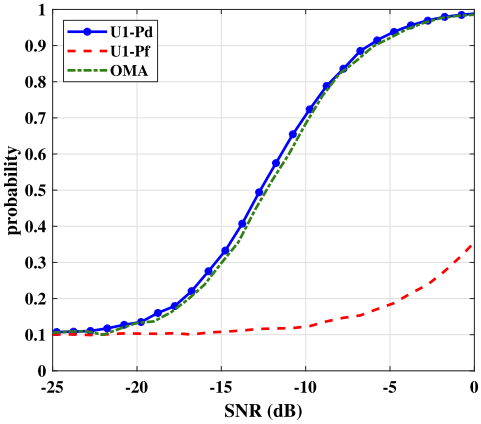

(a) The P_d and P_f of two users with SNR compensation before threshold adjustment.

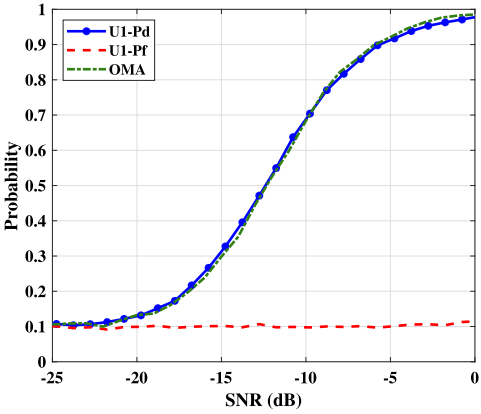

(b) The P_d and P_f of U1 with SNR compensation after threshold adjustment.

Fig. 10. Downlink NOMA system with power allocation $\alpha_1 : \alpha_2 = 2 : 1$, when U2 is keep on transmitting.

4.3 Threshold Adjustment for Mode 2

Now we come up with a numerical solution to adjust the threshold. We use the ratio of the feature amplitude when U1 in H_0 condition to the threshold to adjust the new threshold, the following three pairs of figures (Fig. 9, Fig. 10 and Fig. 11) show the result before and after adjustment.

Figure 9 shows that after threshold adjustment, the curve of P_d is still close to OMA. Especially, around –2–0 dB, the P_d value of U1 is slightly inferior to P_d of OMA. Probably because when U1 is transmitting, the feature amplitude of this situation is significantly greater than the threshold. Even if the threshold is adjusted, it is still quite small for most feature values in the case of H_1.

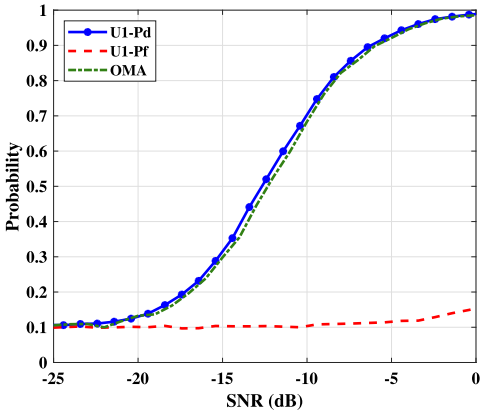

(a) The P_d and P_f of two users with SNR compensation before threshold adjustment.

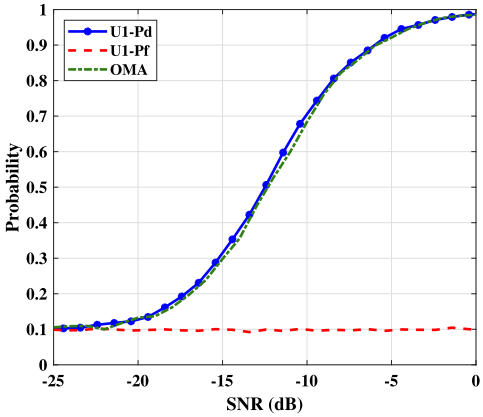

(b) The P_d and P_f of U1 with SNR compensation after threshold adjustment.

Fig. 11. Downlink NOMA system with power allocation $\alpha_1 : \alpha_2 = 10 : 1$, when U2 is keep on transmitting.

Figure 10(a) exhibits that P_f is largely influenced when more power is allocated to U2. The P_f of U1 even reaches to about 0.35 at 0 dB. The adjustment result as Fig. 10(b) indicates, when the power of U2 is relatively high, P_d will significantly decrease at high SNR, which is 0.02 less than OMA at most. When the power of U2 decreases, as shown in Fig. 11(a), P_f also fluctuates less, which is around 0.14 at 0 dB. Hence, as Fig. 11(b) indicates, there was barely changed after the adjustment. This result reveals that the less power is allocated, the less influence has the threshold adjustment on P_d is.

To sum up, this mode of keep U2 transmitting has the P_f that failed to regulate. The method presented in this chapter can solve this problem. Moreover, in this mode with threshold adjustment, the result indicates that the effect on the detection performance of U1 is not particularly obvious.

5 Conclusion

In this paper, we have investigated the application of spectrum sensing in NOMA system. We have designed the workflow and simulated it to verify the feasibility of the scheme. Considering the form of NOMA, we have designed two modes of spectrum sensing, and distinguished the downlink and uplink scenarios in the two modes. Then we have simulated the scenarios and studied the detection performance. The simulation results confirm that the proposed NOMA-spectrum sensing technology has good detection performance, which is attractive for practice.

Our future work will involve more properties of spectrum sensing based on NOMA, improvements in performance, and further applications.

Acknowledgement. The authors' work was supported in part by the Science and Technology Commission Foundation of Shanghai (No. 21511101400), Shanghai Rising-Star Program (No. 21QC1400800), the National Natural Science Foundation of China (No. 61801461) and the Youth Innovation Promotion Association of CAS.

References

1. Zhang, Z., et al.: 6G wireless networks: Vision, requirements, architecture, and key technologies. IEEE Veh. Technol. Mag. **14**(3), 28–41 (2019)
2. Ghosh, A., Maeder, A., Baker, M., Chandramouli, D.: 5G evolution: a view on 5G cellular technology beyond 3GPP release 15. IEEE Access **7**, 127639–127651 (2019)
3. Xu, T., Zhou, T., Tian, J., Sang, J., Hu, H.: Intelligent spectrum sensing: when reinforcement learning meets automatic repeat sensing in 5G communications. IEEE Wirel. Commun. **27**(1), 46–53 (2020)
4. Zou, Z., Yin, R., Wu, C., Yuan, J., Chen, X.: Distributed spectrum and power allocation for D2D-U networks. In: Monami 2020, pp. 161–180. Springer International Publishing, Chiba (2020)
5. Vitturi, S., Zunino, C., Sauter, T.: Industrial communication systems and their future challenges: next-generation ethernet, IIoT, and 5G. Proc. IEEE **107**(6), 944–961 (2019)
6. Chen, S., Zhai, D., Bai, W., Guan, H., Ma, P., Shao, W.: Resource allocation scheme design in power wireless heterogeneous networks considering load balance. In: Monami 2020, pp. 111–124. Springer International Publishing, Chiba (2020)
7. Giordani, M., Polese, M., Mezzavilla, M., Rangan, S., Zorzi, M.: Toward 6G networks: use cases and technologies. IEEE Commun. Mag. **58**(3), 55–61 (2020)
8. Zhang, J., Björnsonon, E., Matthaiou, M., Ng, D.W.K., Yang, H., Love, D.J.: Prospective multiple antenna technologies for beyond 5G. IEEE J. Select. Areas Commun. **38**(8), 1637–1660 (2020)

9. Qu, H., Xu, X., Zhao, J., Yan, F., Wang, W.: A robust hyperbolic tangent-based energy detector with gaussian and non-gaussian noise environments in cognitive radio system. IEEE Syst. J. **14**(3), 3161–3172 (2020)
10. Spooner, C.M., Mody, A.N.: Wideband cyclostationary signal processing using sparse subsets of narrowband subchannels. IEEE Trans. Cogn. Commun. Netw. **4**(2), 162–176 (2018)
11. Cabric, D., Mishra, S., Brodersen, R.: Implementation issues in spectrum sensing for cognitive radios. In: 2004 Conference Record of the Thirty-Eighth Asilomar Conference on Signals, Systems and Computers, vol. 1, pp. 772–776 (2004)
12. Salama, G.M., Taha, S.A.: Cooperative spectrum sensing and hard decision rules for cognitive radio network. In: 2020 3rd International Conference on Computer Applications Information Security (ICCAIS), pp. 1–6 (2020)
13. Sherbin, M.K., Sindhu, V.: Cyclostationary feature detection for spectrum sensing in cognitive radio network. In: 2019 International Conference on Intelligent Computing and Control Systems (ICCS), pp. 1250–1254 (2019)
14. Yasrab, T., Gurugopinath, S.: Spectral efficiency of MIMO-NOMA cognitive radios with energy-based spectrum sensing. In: 2019 IEEE International Conference on Distributed Computing, VLSI, Electrical Circuits and Robotics (DISCOVER), pp. 1–6 (2019)
15. Chin, W.L.: On the noise uncertainty for the energy detection of OFDM signals. IEEE Trans. Veh. Technol. **68**(8), 7593–7602 (2019)
16. Picciolo, M.L., Myrick, W.L., Goldstein, J.S.: A quadrature median matched filter for robust detection and estimation. In: 2019 International Radar Conference (RADAR), pp. 1–6 (2019)
17. Xu, T., Zhang, M., Hu, H., Chen, H.H.: Sliced spectrum sensing-a channel condition aware sensing technique for cognitive radio networks. IEEE Trans. Veh. Technol. **67**(11), 10815–10829 (2018)
18. Saad, W., Bennis, M., Chen, M.: A vision of 6G wireless systems: applications, trends, technologies, and open research problems. IEEE Netw. **34**(3), 134–142 (2020)
19. Yang, P., Xiao, Y., Xiao, M., Li, S.: 6G wireless communications: vision and potential techniques. IEEE Netw. **33**(4), 70–75 (2019)
20. Wang, K., Zhou, T., Xu, T., Hu, H., Tao, X.: Asymmetric adaptive modulation for uplink NOMA systems. IEEE Trans. Commun. **69**, 1–1 (2021)
21. Yang, K., Yang, N., Ye, N., Jia, M., Gao, Z., Fan, R.: Non-orthogonal multiple access: achieving sustainable future radio access. IEEE Commun. Mag. **57**(2), 116–121 (2019)
22. Maraqa, O., Rajasekaran, A.S., Al-Ahmadi, S., Yanikomeroglu, H., Sait, S.M.: A survey of rate-optimal power domain NOMA with enabling technologies of future wireless networks. IEEE Commun. Surv. Tutor. **22**(4), 2192–2235 (2020)
23. Wei, F., Zhou, T., Xu, T., Hu, H.: BER analysis for uplink NOMA in asymmetric channels. IEEE Commun. Lett. **24**(11), 2435–2439 (2020)
24. Ding, Z., Lei, X., Karagiannidis, G.K., Schober, R., Yuan, J., Bhargava, V.K.: A survey on non-orthogonal multiple access for 5G networks: Research challenges and future trends. IEEE J. Select. Areas Commun. **35**(10), 2181–2195 (2017)
25. Wang, Z., Xu, T., Zhou, T., Hu, H.: Joint tier slicing and power control for a novel multicast system based on NOMA and D2D-relay. In: GLOBECOM 2020–2020 IEEE Global Communications Conference, pp. 1–6 (2020)
26. Wang, X., Jia, M., Guo, Q.: Full-duplex cooperative non-orthogonal multiple access with spectrum sensing. In: 2020 15th IEEE International Conference on Signal Processing (ICSP), pp. 411–416 (2020)

27. Liu, X., Wang, Y., Liu, S., Meng, J.: Spectrum resource optimization for NOMA-based cognitive radio in 5G communications. IEEE Access **6**, 24904–24911 (2018)
28. Song, Z., Wang, X., Liu, Y., Zhang, Z.: Joint spectrum resource allocation in NOMA-based cognitive radio network with SWIPT. IEEE Access **7**, 89594–89603 (2019)
29. Jia, M., Wang., X., Guo, Q., Ho, I., Gu, X., Lau, F.: Performance analysis of cooperative non-orthogonal multiple access based on spectrum sensing. IEEE Trans. Veh. Technol. **68**(7), 6855–6866 (2019)
30. Wang, X., et al.: Energy efficiency optimization for NOMA-based cognitive radio with energy harvesting. IEEE Access **7**, 139172–139180 (2019)
31. Bauch, G., Malik, J.: Cyclic delay diversity with bit-interleaved coded modulation in orthogonal frequency division multiple access. IEEE Trans. Wirel. Commun. **5**(8), 2092–2100 (2006)
32. Iradukunda, N., Nguyen, H.T., Hwang, W.J.: On cyclic delay diversity-based single-carrier scheme in spectrum sharing systems. IEEE Commun. Lett. **23**(6), 1069–1072 (2019)